MECHANICS

UDC 621.81/85

THE STRESS–STRAIN STATE IN THE PROCESS OF DEFORMABLE INDENTER PENETRATION INTO THE ELECTROCONDUCTIVE HALF SPACE IN THE PRESENCE OF DISCHARGE CURRENT

A.A. Vantsyan

Institute of Mechanics of NAS RA

The main goal of this work is to study the influence of the discharge current on the characteristic values of penetration. As it has turned out, LRC circuit parameters, the impact velocity, the type of discharge current significantly influence the penetration. However, as experiments and numerical calculations have shown, an important role plays the distance between the target and the plate Δ. It is known that the electron–plastic effect depends on the current value, direction of $\vec{J}$, as well as the current exposure time. It follows that the distance of the plate from the target also influences the electron–plastic effect, which occurs in the penetrating indenter on the segment between the contact surface of the deformed indenter with the crater and the plate, with a crater. Because the length of the segment affects the closed LRC circuit time, and which, in its turn, affects the time of discharge current on the plastic properties of the indenter, as well as the duration of the Ampere force $\vec{J} \times \vec{H}$ as a pinch–effect becomes essential.

From a practical point of view, it is important to study the problem of the indenter (jump) rebound from the crater. For this purpose, approximate estimates were carried out in [1] for the deformable indenter. The (jump) rebound of the indenter may occur due to the fact that after stopping the indenter in a half–space or in the case when the depth of penetration is less than the thickness of the target, in the target, due to the elastic, (stored) accumulated in the indenter and the target stresses, the reverse motion of the indenter takes place. Thus, if the friction forces between the indenter and the target are less critical, a (jump) rebound of the indenter from the crater occurs. This phenomenon was observed at the experiments, when the barrier was shot in the presence of the current. The blunting of the indenter and the pressing force in the target create favorable conditions for rebound.

Keywords: penetration, stress–strain, indenter, electro-conductive, discharge current.

Introduction. To the problem of penetration of thin rigid or deformable bodies into initially elastic media are devoted many works. On the basis of the plate section theory, early determination of stress–strain state in the indenter and media is carried out. In the last ten years the influence of discharge currents on the penetration

processes has been investigated by me. In particular, the essential phenomena of the influence of discharge currents on the penetration phenomena have been discovered theoretically. As shown in previous works, the action of the discharge current on the mechanical parameters of penetration are large. It was experimentally and theoretically shown that the discharge currents lead to an essential degree of the penetration depth.

Investigation methods. In the present article, the characteristic equations of the penetration phenomena are solved numerically.

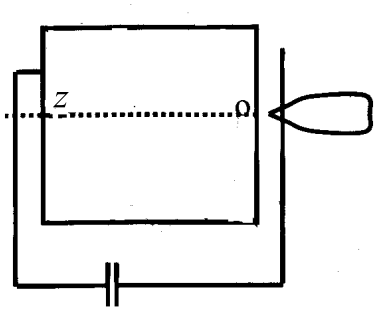

Fig.1. The principal scheme of penetration

The study of the impact of the discharge current on the process of penetration, in particular, on the depth of penetration and the shape of the indenter and the crater was conducted experimentally in [1,2] Fig.1.

In this article, a numerical calculation is conducted to investigate the stress–stain state of the indenter and the crater, where the process of penetration is accompanied by the discharge current.

A detailed analysis of the influence of parameters of the LRC circuit on the indenter shape, the crater and the free surface, as well as on the shape of the equipotential surfaces of the stresses $\sigma_{rr}, \sigma_{zz}, \sigma_{\theta\theta}$ is presented. Is The numerical solution confirms the effect observed by experimentation in [2], – a significant decrease in the depth of the indenter penetration in the conductive half–space in the presence of the discharge current. Numerical calculations were carried out for different values of the L,R,C parameters, as well as different distances between the half–space and plate set before the half–space.

Taking into account the axis–symmetric problem, to the system of equations that includes conservation equations of mass, momentum and energy, should be added the induction equation, then the equation takes the form:

$$\frac{\partial}{\partial t}(Ur) + \frac{\partial}{\partial r}(Fr) + \frac{\partial}{\partial z}(Gr) + Hr = 0 \,(1),$$

where U, F, G are given by (1), and H takes the form:

$$\bar{U}=\begin{Vmatrix}\rho\\ \rho u\\ \rho v\\ e\end{Vmatrix},\quad \bar{F}=\begin{Vmatrix}\rho u\\ \rho u^2-\sigma_r\\ \rho uv-\sigma_{rz}\\ (e-\sigma_r)u-\sigma_{rz}v\end{Vmatrix},\quad \bar{G}=\begin{Vmatrix}\rho v\\ \rho uv-\sigma_{rz}\\ \rho u^2-\sigma_r\\ (e-\sigma_z)v-\sigma_{rz}u\end{Vmatrix},$$

$$H=\begin{Vmatrix}0\\ -\mu_0 j_z H_\theta+\dfrac{\sigma_\theta}{r}\\ \mu_0 j_r H_\theta\\ \dfrac{\mu_0\mu}{2}\cdot\dfrac{\partial H_\theta^2}{\partial t}+\dfrac{j_z^2}{\bar{\sigma}}-\dfrac{j_z\mu H_\theta}{\bar{\sigma}}+\dfrac{j_r^2}{\bar{\sigma}}-\dfrac{j_r\nu H_\theta}{\bar{\sigma}}\\ -\dfrac{\partial(\nu H_\theta)}{\partial z}-\dfrac{\partial(uH_\theta)}{\partial r}+\dfrac{1}{\bar{\sigma}\mu_0\mu}\left\{\dfrac{1}{r}\dfrac{\partial}{\partial r}\left(r\dfrac{\partial H_\theta}{\partial r}\right)+\dfrac{\partial^2 H_\theta}{\partial z^2}-\dfrac{H_\theta}{r^2}\right\}\end{Vmatrix},$$

u, v – particle velocities in the medium along the axes of r, z; $\sigma_r=\sigma+s_r$, $\sigma_z=\sigma+s_z$, $\sigma_\varphi=\sigma-(s_r+s_z)$, $\sigma_{rz}=s_{rz}$ – components of the stresses tensor

$$j_z=\frac{1}{r}\frac{\partial(rH_\theta)}{\partial r},\ j_r=\frac{\partial H_\theta}{\partial z},\ e=\rho\left[\varepsilon+\frac{1}{2}(u^2+v^2)-\frac{1}{2}\mu_0 H_\theta^2\right].$$

Boundary conditions for j_z are given in the form $j_z=j_r=0$, for $r>r_0$; while for $r\le r_0$ $j_z(t)$ are given as a solution to (1), r_0 is the initial radius of the indenter contact with the target.The problem was numerically solved for penetrating curvilinear nose shape, cylinder shape and sphere bodies.

The purpose of numerical calculations was to find the maximum depth of penetration of the indenter, forms of the indenter and the crater with a free surface, the location of the plastic front in the half–space and in the indenter for various values of L,R,C during the process of penetration.

Calculations were made for the indenter with length of $l_0=10^{-1}\,m$, initial radius of the cylindrical part of $r_0=45\cdot10^{-4}\,m$ with different initial impact velocities and with different gaps between the target and the plate.

Numerical calculations were performed for the following values of the constants:

Parameters of the target:

$\sigma_s=3\cdot10^8\,N/m^2$, $\rho_0=2700\,kg/m^3$, $\mu=7\cdot10^{11}\,N/m^2$,

$a_1=-1.53\cdot10^{11}\,N/m^2$, $a_2=-1.74\cdot10^{11}\,N/m^2$,

$a_3=-0.532\cdot10^{11}\,N/m^2$, $a_4=-1.912$, $a_5=0.386$.

Parameters of the indenter:

$\sigma_s = 3 \cdot 10^9\, N/m^2,\ \rho_0 = 2700\, kg/m^3,\ \mu = 7 \cdot 10^{12}\, N/m^2,$

$a_1 = -1.53 \cdot 10^{12}\, N/m^2,\ a_2 = -1.74 \cdot 10^{12}\, N/m^2,$

$a_3 = -0.532 \cdot 10^{12}\, N/m^2,\ a_4 = -1.912,\ a_5 = 0.386.$

Investigation results. Values of the L,R,C parameters and the initial impact velocity are shown in the figures. Fig. 2,3 show the stress–strain state of the target and the indenter, the indenter shape and the free surface.

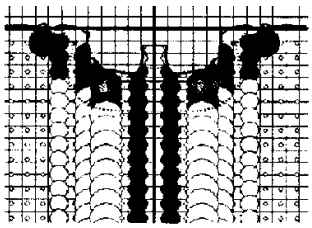

Fig.2. A body with a curvilinear fore part, field σ_{rr}

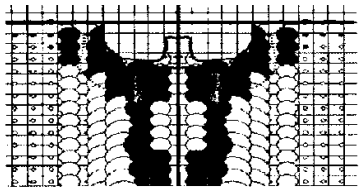

Fig.3. A body with a curvilinear fore part, field σ_{zz}

$$V_0 = 720\text{m/sec}.\ I_0 = 10^5 \frac{A}{\text{m}^2\,\text{sec}.},\ L = 7 \cdot 10^{-8}\,\text{Hn},\ R = 0.001O\text{m},\ C = 0.02F$$

$$t = 3.6 \cdot 10^{-5}\, mc\ sec$$

In Figures 6,7 are introduced similar pictures for the case of penetration in the absence of discharge current. Looking at the penetration pictures, and comparing the cases when there is $J \neq 0$ and there is no $J = 0$ discharge current, it is easy to see that a significant decrease in the depth of penetration of the indenter due to the discharge current occurs. The presence of current also leads to a spatial distribution of stresses $\sigma_{rr}, \sigma_{zz}, \sigma_{\theta\theta}$, as well as to a significant increase in plastic deformation of the indenter and the target in the radial direction. Comparing the radius of the circles, proportional to the corresponding stresses, we can easily notice that the discharge current leads to an increase of the stress values compared with the case $J = 0$. This can be explained by the Pinch effect, which as Ampere force $\bar{F}_A = \bar{J} \times \bar{H}$ leads to the compression (pressing) of the medium generating additional stresses.

Observing the picture regarding the penetration time, you will notice the stress waves propagating in r and z. The wave in r is much more noticeable. The wave dynamics is also observed in the indenter, which vibrates both in radial and axial directions.

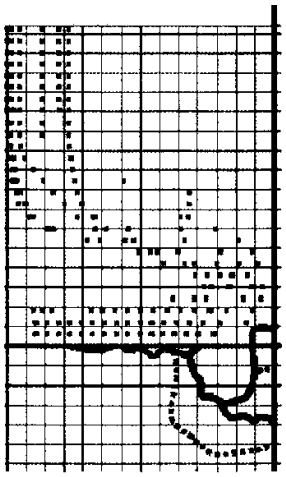

Fig.4. Ilustriation of the fragments

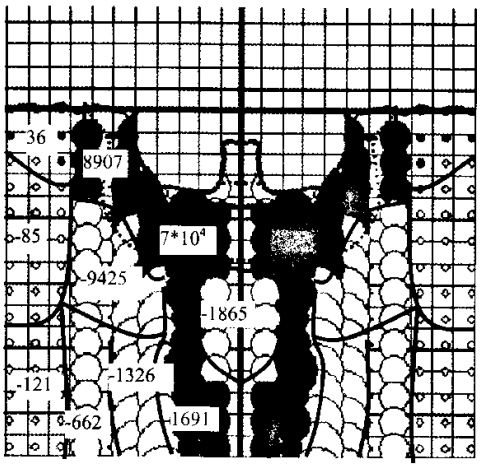

Fig. 5. Field σ_{zz}, $t = 3.6 \cdot 10^{-5}$ mc sec

$V_0 = 720\text{m/sec}. I_0 = 10^5 \frac{A}{\text{m}^2\,\text{sec}.}$, $L = 7 \cdot 10^{-8}$ Hn, $R = 0.001O\text{m}$, $C = 0.02F$

t=2.1·10^{-5} *mc sec* Equipotential surfaces

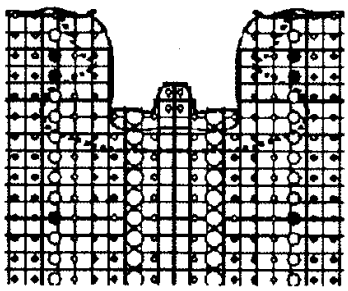

Fig.6. A body with a curvilinear fore part, field σ_{rr}

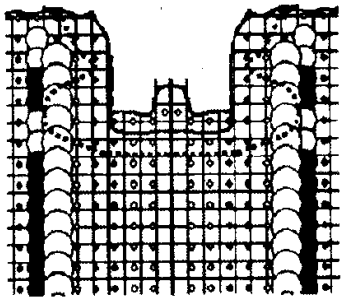

Fig.7. A body with a curvilinear fore part, field σ_{zz}

t=3·10 $^{-5}$ *mc sec*

In Figures 4, fragments flying off the free surface of the target and from the crater are shown. The presence of the fragments is a consequence of the impact of the indenter and the target, but mostly it is noticeable in the presence of the discharge current. Fragments were determined calculating the density of the medium in the region $z < 0$.

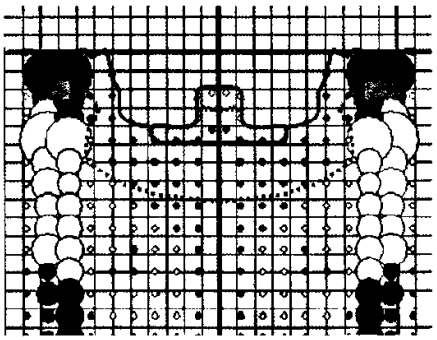

Fig. 8. A body with a curvilinear fore part, field σ_{zz}

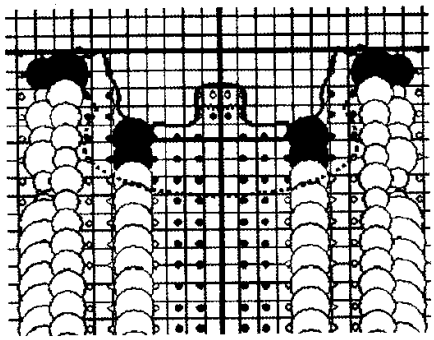

Fig. 9. A body with a curvilinear fore part, field σ_{rr}

$t = 32 \cdot 10^{-6}$ *mc sec*

To study the influence of the capacitor's energy on the phenomena of the penetration depth decrease, experiments [1] and numerical calculations for different values of the capacitor capacitywere performed. Figs. 8,9 show the corresponding values at $C = 0.004\,\mathrm{F}$ and other identical parameters Figs.8,9 show the little difference of depth decrease of penetration compared with the case $C = 0.02\,\mathrm{F}$. A similar effect is also observed during the experiments.

However, there is a significant difference in the stress state pictures for the same time periods of the penetration process. In particular, it can be seen from Figs. 2-9 for stresses σ_{rr} and σ_{zz} at $t = 36 \cdot 10^{-6}\,\mathrm{sec}$.

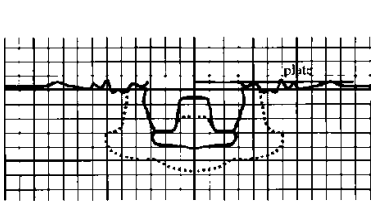

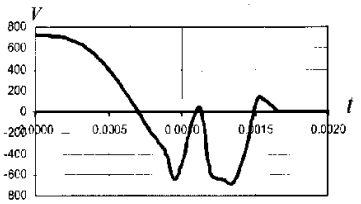

Fig. 10. A body with a curvilinear fore part

Fig. 11. The dependence of the penetration velocity from the time

$t = 1.74 \cdot 10^{-4}$ *mc sec*

At various capacitor capacities, a slight difference in the fragments pictures is observed.

With a view to designing (projection) of targets it is of interest to determine the surfaces of the same values of the stresses – the equipotential surfaces.

Fig. 5 also shows equipotential surfaces for the stress σ_{zz} with appropriate parameter values.

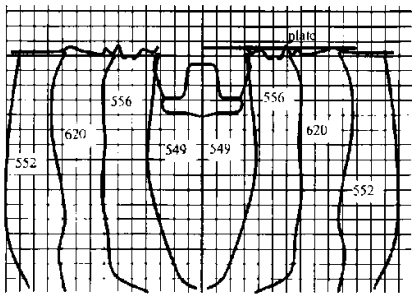

Fig. 12.The distribution of the inner energy $t = 1.74 \cdot 10^{-4}$ *mc sec*

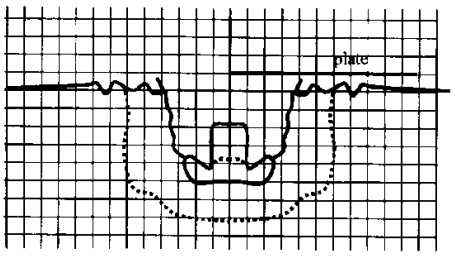

Fig. 13.A body with a curvilinear fore part $t = 1.86 \cdot 10^{-4}$ *mc sec*

To study the influence of the indenters` shape, indenters of cylinder shape and sphere shape were numerically considered. It is made similar to the previous case pictures for the indenters of cylinder and sphereshapes.

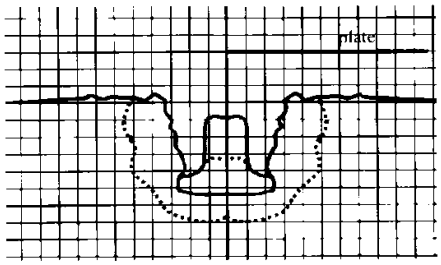

Fig.14. A body with a curvilinear fore part t=2.16·10^{-4} mc sec

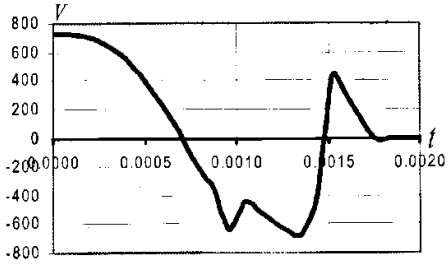

Fig.15. The dependence of the penetration velocity from the time

Comparing the pictures at the stopping time of the indenter, it can be seen that the depth of penetration of the cylinder is ~20% less compared with the depth of penetration of the curvilinear body. There isalso a difference in the stress state.

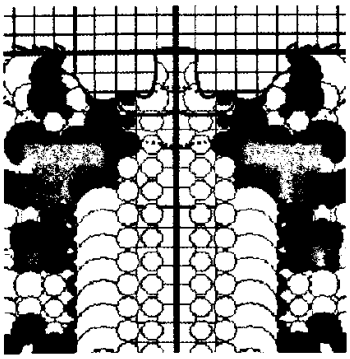

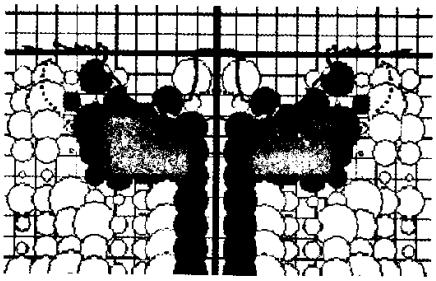

Fig. 16. Body cylinder, field σ_{rr} *Fig. 17. Body cylinder, field* σ_{zz}

$t=3.2\cdot10^{-5}$ *mc sec*

Figs. 18, 22 show the impact fragments of a cylindrical body and the targets.

The influence of the capacitor energy was also investigated in the case of penetration of a cylindrical indenter, Figures 16,17,20,21 show the stress–strain state pictures.

In Figs. 19,23 the equipotential surfaces of stresses in the process of penetration of a cylindrical indenter at the time $t=3.8\cdot10^{-6}$ *mc sec* is shown.

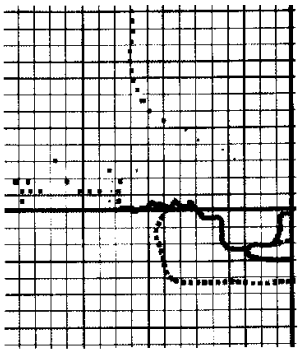

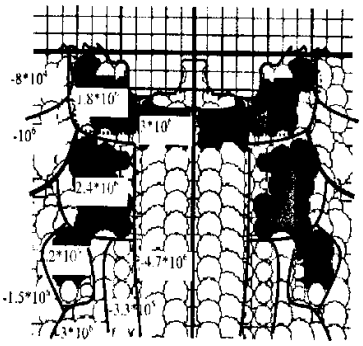

Fig. 18. The illustrations of the fragments *Fig. 19.* Field σ_{rr},

$t=3.8\cdot10^{-5}$ *mc sec*

From a practical point of view, the problem of penetration of the indenter of the sphereshape is of interest. Figs. 24, 25 are made similar to the previous problems, the values characterize the process of penetration of a deformable indenter.

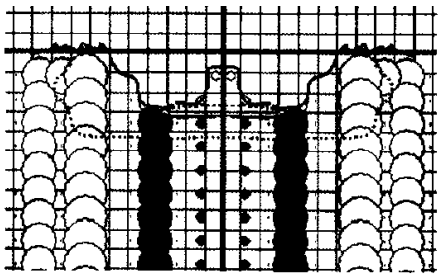

Fig. 20. Body cylinder, field σ_{rr}
$t = 4 \cdot 10^{-5} mc\ sec$

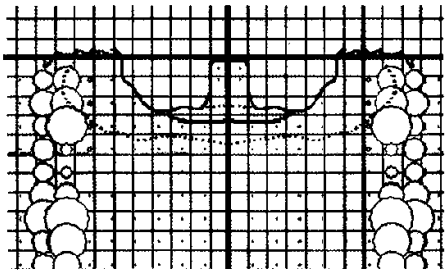

Fig. 21. Body cylinder, field σ_{zz}
$t = 3 \cdot 10^{-5}\ mc\ sec$

Comparing the stress–strain state graphs in the problem of penetration of the sphere, one can conclude that the discharge current has little effect on the process of penetration. This can be explained by the fact that the characteristic dimension of thesphere in the direction of penetration, i.e. the diameter is much smaller than the length of the cylindrical indenter, so the time of the closed circuit (chain) LRC for the sphere is much less than the same time for a cylindrical indenter, which in its turn, leads to the small influence of the discharge current.

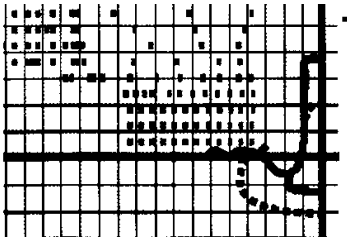

Fig. 22. The illustration of the fragments.
$t = 5 \cdot 10^{-6}\ mc\ sec$

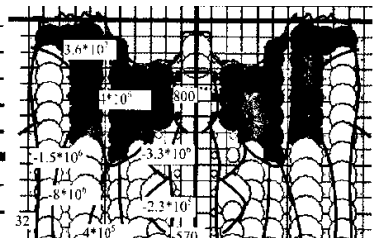

Fig.23. Field σ_{zz},
$V_0 = 720 \text{m/sec}. I_0 = 10^5 \frac{A}{\text{m}^2 \text{sec}.}, \ L = 7 \cdot 10^{-8} \text{Hn}, \ R = 0.001 \text{Om}, \ C = 0.004 F$
$t = 4 \cdot 10^{-5}\ mc\ sec$

However, from the Figures of the crater and indenter, it can be seen that their forms in the absence and the presence of discharge current differ very much. In the presence of discharge current, the crater has a smoother form (appearance), and the free surface of the target is wavier. The characteristic dimensions of the plastic regions for the cases are identical, although the form of plastic surfaces is also significantly different.

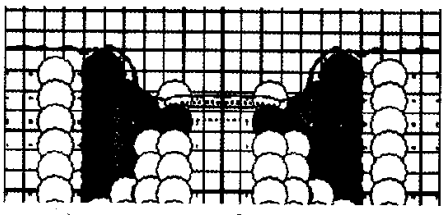

Fig. 24. Body sphere, field σ_{rr} surfaces

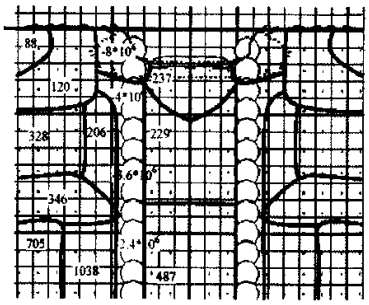

Fig.25. Body sphere, field σ_{zz} Equipotential

$$V_0 = 720\text{m/sec}.\, I_0 = 10^5 \frac{A}{\text{m}^2\,\text{sec}.},\ L = 7\cdot 10^{-8}\text{Hn},\ R = 0.001\text{Om},\ C = 0.02F$$

$$t = 3.6\cdot 10^{-5}\ mc\ sec$$

From a practical point of view, it is important to study the problem of the indenter (jump) rebound from the crater. For this purpose, approximate estimates were carredout in [1] for the deformable indenter. The (jump) rebound of the indenter may occur due to the fact that after stopping the indenter in a half–space or in the case when the depth of penetration is less than the thickness of the target, in the target due to the elastic, (stored) accumulated in the indenter and the target stresses, the reverse motion of the indenter takes place. Thus if the friction forces between the indenter and the target are less critical, a (jump) rebound of the indenter from the crater occurs. This phenomenon was observed at the experiments, when the barrier was shot in the presence of the current. The blunting of the indenter and the pressing force in the target create favorable conditions for rebound. Figs. 11,15 show the dependence of $V(t)$ in the process of penetration. It is clearly shown that after stopping, the indenter obtains a negative velocity. Figs. 6,7 show that the vibration of the indenter around the maximum depth occurs. After some time, the velocity becomes zero, the indenter stops, so there is no rebound.

For this purpose, numerical calculations for different values of Δ were performed. Figures 10,12,13,14 show the pattern of penetration of the deformable indenter for the same values of V,L,R,C but a different Δ. As the Figures show, the maximum depth experimentally depends on Δ. If compared with Fig. 10, in Figure 13, Δ is doubled, and at the same time, a 20…25%, decrease in the depth of penetration is observed, then with the further increase of Δ (Fig.14), an increase in the depth of penetration is observed or, what is the same (equivalently), a decrease in the electron–plastic effect. This is due to the insufficient utilization of the capacitor energy, as in the latter case, interruption of the circuit occurs earlier than in the previous case. The analysis of the graphs shows that the shape of the plastic front and

free surface also depend on Δ. It is evident that the greater the decrease in the depth of penetration is, the greater the waviness of the free surface is.

Conclusion. In conclusion, it may be noted that in this article, the impact problem of two deformable media accompanied by discharge current has reached a qualitatively new level. In the process of studying this problem, in addition to the main result, a decrease in the penetration depth of the indenter in the target at the cost of discharge current, qualitatively new results were obtained in physics of discharge processes.

It should also be noted that the results of this study may serve as a basis for creating a more impact–resistant target in the military industry.

References

1. **Vantsyan A.A.** Influence of discharge current on the perforation of plates.- Moscow: Nauka, 2012.- 287p.
2. **Vantsyan A.A.** Influence of the electromagnetic field and anisotropic properties of the media on the dynamic processes in continuous media. - Yerevan: Gitiutyn, 2004. - 224p.

Received on 01.11.2018.
Accepted for publication on 18.12.2018.

ԷԼԵԿՏՐԱՀԱՂՈՐԴԻՉ ԿԻՍԱՏԱՐԱԾՈՒԹՅԱՆ ՄԵՋ ՁԵՎԱԽԱԽՏՎՈՂ ԻՆԴԵՆՏՈՐԻ ՄԽՐՃՄԱՆ ԸՆԹԱՑՔՈՒՄ ԿԻՍԱՏԱՐԱԾՈՒԹՅՈՒՆՈՒՄ ԼԱՐՎԱԾԱԴԵՖՈՐՄԱՑԻՈՆ ՎԻՃԱԿԸ ՊԱՐՊՄԱՆ ՀՈՍԱՆՔԻ ԱՌԿԱՅՈՒԹՅԱՆԴԵՊՔՈՒՄ

Ա.Ա. Վանցյան

Ուսումնասիրվում է մխրճման բնութագրիչների վրա պարպման հոսանքի ազդեցությունը, մասնավորապես՝ LRC շղթայի բնութագրիչների, հարվածի արագության, հոսանքի պարպման տեսքը: Կարևոր դեր է խաղում նաև թիրախի և նրա դիմաց գտնվող թիթեղի միջև եղած հեռավորությունը: Հայտնի է, որ էլեկտրոնա–պլաստիկության երևույթը կախված է հոսանքի արժեքից, հոսանքի ուղղությունից, ինչպես նաև հոսանքի ազդման ժամանակից: Անհրաժեշտ է նշել, որ թիրախում լարվածադեֆորմացիոն վիճակը կախված է թիրախի և թիթեղի միջև եղած հեռավորությունից, և քանի որ մխրճվող մարմնի երկարությունն ազդում է LRC շղթայի պարպման ժամանակի վրա, ուստի պարպման հոսանքի ազդեցությունը մխրճվող մարմնի պլաստիկական հատկությունների, ինչպես նաև ամպերյան ուժի վրա դառնում է կարևոր: Կիրառական տեսակետից կարևոր է ուսումնասիրել ինդենտորի հետընթաց շարժումը խարանի միջից:

Աշխատանքում տրված է ձևախախտվող ինդենտորի հետշարժման մոտավոր գնահատականը: Ինդենտորի հետշարժումը սկսվում է նրա լրիվ կանգից հետո կիսատարածության մեջ կամ եթե մխրճման խորությունը փոքր է արգելքի հաստությունից: Առաձգական ուժերը ինդենտորը շարժում են հակառակ ուղղությամբ, այսինքն՝ եթե ինդենտորի և խարանի միջև առաջացած շփման ուժերը փոքր են կրիտիկական արժեքից, ապա տեղի է ունենում ինդենտորի հետշարժումը խարանի միջից: Այս երևույթը նկատվել է փորձարարական ճանապարհով, երբ մխրճման պրոցեսը տեղի է ունեցել պարպման հոսանքի առկայության դեպքում: Ինդենտորի բթացումը և սեղմող ուժերի առկայությունը վկայում են այդ մասին:

Առանցքային բառեր. մխրճում, լարվածադեֆորմացիոն վիճակ, ինդենտոր, էլեկտրահաղորդականություն, պլաստիկություն, պարպման հոսանք:

НАПРЯЖЕННО–ДЕФОРМИРОВАННОЕ СОСТОЯНИЕ В ПРОЦЕССЕ ПРОНИКНОВЕНИЯ ДЕФОРМИРУЕМОГО ИНДЕНТОРА В ЭЛЕКТРОПРОВОДЯЩЕЕ ПОЛУПРОСТРАНСТВО ПРИ НАЛИЧИИ РАЗРЯДНОГО ТОКА

А.А. Ванцян

Изучается влияние разрядного тока на характеристики проникновения, в частности, параметры цепи LRC, скорость удара, тип разряда. Однако, как показывают эксперименты и численные расчеты, важную роль играет расстояние между мишенью и пластиной. Известно, что электронно–пластический эффект зависит от значения тока, направления J, а также от времени действия тока. Следует также отметить, что электронопластичность в мишени зависит от расстояния между пластиной и мишенью. Так как длина индентора влияет на время замыкания цепи LRC, то влияние разрядного тока на пластические свойства индентора, а также протяженность амперовой силы $\vec{J} \times \vec{H}$ в качестве Панч–эффекта становится существенным.

С точки зрения практики, важно изучить задачу отскока индентора из кратера.

В настоящей статье дана приближенная оценка для деформируемого индентора. Отскок индентора имеет место после остановки в полупространстве или в случае, когда глубина проникновения меньше толщины преграды. Упругие напряжения двигают индентор в обратном направлении, т.е. если силы трения между индентором и среды меньше критического значения, имеет место отскок индентора из кратера. Это явление наблюдалось экспериментальным путём, когда проникновение индентора происходило при наличии тока. Затупление индентора и сжимающие силы в преграде являются условием отскока.

Ключевые слова: проникновение, напряженно–деформированное состояние, индентор, электропроводность, пластичность, разрядный ток.